Striking Stabilization of Arc Repressor by an Engineered Disulfide Bond†

Clifford R. Robinson‡ and Robert T. Sauer*

Department of Biology, Massachusetts Institute of Technology, Cambridge, Massachusetts 02139

Received June 28, 2000; Revised Manuscript Received August 4, 2000

ABSTRACT: A solvent-exposed Cys11−Cys11′ disulfide bond was designed to link the antiparallel strands of the β sheet both in the Arc repressor dimer and in a single-chain variant in which the Arc subunits are connected by a 15-residue peptide tether. In both proteins, the presence of the disulfide bond increased the T_m by approximately 40 °C. In the single-chain background, the disulfide bond stabilized Arc by 8.5 kcal/mol relative to the reduced form, a significantly larger degree of stabilization than caused by other engineered disulfides and most natural disulfides. This exceptional stabilization arises from a modest effective concentration of the Cys11−Cys11′ disulfide in the native state (71 M) and an anomalously low effective concentration in the denatured state (40 μM). Disulfide cross-linking of the two β strands in the single-chain Arc background accelerated refolding by a factor of 170 into the sub-microsecond time scale. However, the major energetic effect of the disulfide occurs after the transition state for Arc refolding, slowing unfolding by 200 000-fold.

Mutations that increase protein stability provide valuable insights into the determinants of protein folding and stability. We have been studying the effects of mutations on the folding and stability of the Arc repressor dimer of bacteriophage P22 (*1*). The native Arc dimer has a simple fold, consisting of an antiparallel β sheet and four α helices (*2*−*4*). Because both subunits intertwine and contribute to a single hydrophobic core, Arc does not fold stably as a monomer. Thus, native dimerization is coupled to folding, and global stability increases with protein concentration (*5*). Increasing the stability of native Arc by increasing its concentration is limited, however, because denatured Arc also dimerizes at high protein concentrations (*6*).

There are two general classes of amino acid substitutions that enhance protein stability: those that introduce stabilizing interactions or remove destabilizing interactions in the native structure, and those that reduce the entropy of folding by restricting the number of conformations available to the denatured polypeptide chain (*7*). The PL8 mutation of Arc, an example of the first class, permits formation of an additional hydrogen bond at each end of Arc's two-stranded antiparallel β sheet and increases the stability of the mutant dimer by 2.5 kcal/mol (*8*, *9*). This stability increase arises almost exclusively from a decrease in the unfolding rate, suggesting that hydrogen bonding in the β sheet is a late event in Arc folding. The second class includes sequence changes that cross-link different parts of the native structure (*10*−*17*). For example, in the single-chain variant Arc-L1-Arc (herein called sc-Arc), a 15-residue linker connects the C-terminus of one subunit to the N-terminus of the other subunit and stabilizes the protein by increasing the refolding rate (*18*).

In principle, connecting the subunits of the Arc dimer with a disulfide could be far more effective than a peptide linker in increasing protein stability because the disulfide is a more rigid cross-link. Here, we demonstrate that a designed Cys11−Cys11′ disulfide bond in the Arc β sheet does provide a large increase in the thermodynamic stability of this protein to denaturation. In the context of sc-Arc (Arc-L1-Arc), the Cys11−Cys11′ disulfide increased stability by 8.5 kcal/mol, a value roughly twice that of the most successful examples of other engineered disulfides and larger than almost all natural disulfides. The Cys11−Cys11′ disulfide displayed a modest effective concentration of 71 M in the native state and is hyper stabilizing largely because of an anomalously low effective concentration of 40 μM in the denatured state. The dominant kinetic contribution of the Cys11−Cys11′ disulfide to Arc stability occurred between the transition state and the native state, decreasing the unfolding rate by more than 5 orders of magnitude.

MATERIALS AND METHODS

Molecular Biology. DNA oligonucleotides were synthesized using an Applied Biosystems 381A DNA synthesizer and were purified by polyacrylamide gel electrophoresis using standard procedures (*19*). Double-stranded cassettes were annealed by mixing equimolar amounts of the complementary oligonucleotides, heating to 90 °C for 5 min, and cooling slowly. To generate the gene encoding the Arc-NC11 protein, a cassette with the sequence

```
5′ tc gag gtg aat ATG AAA GGA ATG AGC AAA
3′     c cac tta TAC TTT CCT TAC TCG TTT

ATG CCG CAG TTC TGT CTG AGG TGG CCG C 3′
TAC GGC GTC AAG ACA GAC TCC ACC GG   5′
```

† Supported by NIH Grant AI-15706 and by an NIH/NRSA postdoctoral fellowship (GM-61727) to C.R.R.

* Address correspondence to this author at MIT 68-571, 77 Massachusetts Ave., Cambridge, MA 02139. Phone: 617-253-3163; fax: 617-258-0673; e-mail: bobsauer@mit.edu.

‡ Present address: 3-Dimensional Pharmaceuticals, 665 Stockton Dr., Suite 104, Exton, PA 19341. E-mail: robinson@3dp.com.

10.1021/bi001484e CCC: $19.00
Published on Web 09/15/2000

was constructed. The codon for Cys11 is underlined, and upper case letters indicate bases from the coding region of the *arc* gene. This cassette was subcloned between the unique *Xho*I and *Sac*II sites in the pSA700 plasmid vector that encodes wild-type Arc. Mutants were identified by screening for loss of restriction cleavage with *Bsi*36I, as this site is present in wild type but absent in the mutant.

A gene containing the NC11 substitution in each subunit of sc-Arc (designated sc-Arc-NC11) was constructed in three steps. First, the cassette shown above was subcloned into plasmid pLA11A (containing the first Arc subunit and the first half of the linker) to produce plasmid pLA11A-NC11. Plasmid pLA11B-NC11 [containing the second half of the linker, the second Arc subunit, and the *st11* tail sequence (His-His-His-His-His-His-Lys-Asn-Gln-His-Glu; ref *20*)] was constructed by cloning a cassette with the sequence

```
5′ tc gag atg ggt acc ggt ggc ggc tcc gga
3′      c tac cca tgg cca ccg ccg agg cct

 ggc ggc ATG AAA GGA ATG AGC AAA ATG CCG
 ccg ccg TAC TTT CCT TAC TCG TTT TAC GGC

 CAG TTC TGT CTG AGG TGG CCG C 3′
 GTC AAG ACA GAC TCC ACC GG   5′
```

between the unique *Xho*I and *Sac*II sites of plasmid pSA700. Finally, plasmid pLA110-scNC11 was constructed by subcloning the *Kpn*I−*Cla*I fragment from pLA11B-NC11 (containing the linker portion and second Arc repeat) between the unique *Kpn*I and *Cla*I sites of pLA11A-NC11. The DNA sequence encoding each construct was determined using the dideoxy sequencing method (*21*). The genes encoding each of the Arc variants used here are under transcriptional control of a *tac* promoter.

The repressor activities of the Arc-NC11 and sc-Arc-NC11 proteins in vivo were assayed in *Escherichia coli* strain UA2F, using a streptomycin resistance assay (*22*). Equilibrium binding to a 31 bp DNA duplex containing the wild-type *arc* operator was assayed by gel-mobility shift techniques as described (*23, 24*).

Protein Purification. Arc variants were purified to homogeneity using chromatography on Ni−NTA agarose (Qiagen) as described (*20, 24*). Fluorescence spectroscopy and circular dichroism (CD) spectroscopy were also performed as described in these references. To fully reduce Arc-NC11 protein, samples were incubated at 100 °C, pH 2, with 100 mM dithiothreitol (DTT) for 60 min. To completely reduce sc-Arc-NC11 protein, samples were incubated at 100 °C, pH 2, with 100 mM DTT and 8 M urea for 60 min. To produce uniformly oxidized preparations of Arc-NC11 or sc-Arc-NC11, protein samples were reduced by incubation with 100 mM DTT at 90 °C for 10 min (pH 7.5), slowly cooled, and then dialyzed at room temperature against buffer [50 mM Tris-HCl (pH 7.5), 250 mM KCl, 0.2 mM EDTA] without DTT for 48 h to allow air oxidation and formation of the disulfide bond in the native protein. During oxidation, the protein concentration was kept below 10 μM, to minimize formation of intermolecular disulfide bonds. Oxidized protein samples were concentrated using Centricon concentrators (Amicon).

Protein Stability. Stability to guanidine or thermal denaturation was assayed by monitoring changes in the intrinsic tryptophan fluorescence or CD ellipticity at 234 nm using protein samples at concentrations of 10 μM in subunit equivalents (*6, 18*). Denaturation experiments were performed in buffers containing 250 mM KCl, 0.2 mM EDTA, and either 50 mM Tris-HCl (pH 7.5) or 50 mM sodium acetate (pH 2.0); 10 mM DTT was also included in these buffers for experiments with reduced Arc-NC11 or reduced sc-Arc-NC11. Thermodynamic parameters (ΔG_u, m, T_m, and ΔH_u) were obtained by nonlinear least-squares fitting of guanidine or thermal denaturation data to a two-state model (*5, 18*). For fitting of thermal denaturation experiments, ΔC_p was fixed at a value of 1.31 kcal/(mol·deg) as previously reported for Arc and a large set of Arc variants (*25*), but the fitted values of T_m were found to be relatively insensitive to changes in ΔC_p between 1.0 and 1.5 kcal/(mol·deg).

Equilibrium constants for the disulfide−sulfhydryl exchange reactions between glutathione (GSH or GSSG) and the denatured state of the protein (P_{SS} or P_{SH}) for Arc-NC11 (eq 1) or sc-Arc-NC11 (eq 2) were measured using the method of Lin and Kim (*26*).

$$P_{SS} + 2GSH \leftrightarrow 2P_{SH} + GSSG;$$
$$K_{ex} = [P_{SS}][GSH]^2/[P_{SH}]^2[GSSG] \quad (1)$$

$$P_{SS} + 2GSH \leftrightarrow P_{SH} + GSSG;$$
$$K_{ex} = [P_{SS}][GSH]^2/[P_{SH}][GSSG] \quad (2)$$

Briefly, the proteins at 5−50 μM concentrations were denatured in a buffer containing 50 mM Tris-HCl (pH 7.5), 250 mM KCl, 0.2 mM EDTA, and 6 M GuHCl and were incubated with mixtures of reduced and oxidized glutathione at 2−200 mM concentrations to produce varying ratios of reduced and oxidized proteins. After equilibration for 2 h at 25 °C, the reaction mixtures were loaded onto a reverse-phase HPLC column (Whatman C18), and the reduced and oxidized protein species were separated using a gradient from 0 to 40% acetonitrile in 0.1% trifluoroacetic acid. The peak areas corresponding to the reduced and oxidized proteins were quantified by integration (Shimadzu).

Unfolding and Refolding Kinetics. Stopped-flow kinetic experiments of protein folding and unfolding at 25 °C were monitored by changes in fluorescence at protein concentrations between 1 and 10 μM in a buffer containing 50 mM Tris-HCl (pH 7.5), 250 mM KCl, 0.2 mM EDTA, and different concentrations of GuHCl. Unfolding was initiated by denaturant−jump experiments (mixing ratio 1:5) to yield a final GuHCl concentration between 4 and 7 M. Refolding was initiated by mixing protein denatured in 5−7 M GuHCl with low-guanidine buffer (1:5 ratio) to yield final GuHCl concentrations between 0.5 and 4 M. Rate constants were obtained by fitting the kinetic data to single-exponential equations for sc-Arc, disulfide-bonded Arc-NC11, and disulfide-bonded sc-Arc-NC11. For wild-type Arc, refolding data were fit to a hyperbolic equation, and unfolding data were fit to a single-exponential function (*25*). In all cases, the residuals of the fits were found to be randomly distributed.

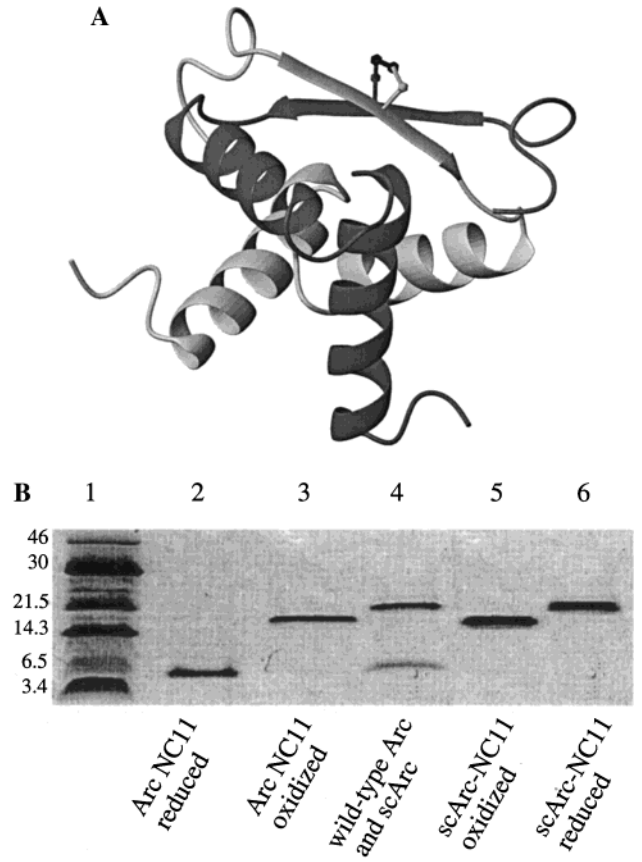

FIGURE 1: (A) Ribbon model of disulfide-linked Arc-NC11. One Arc subunit is colored light gray, the other dark gray. The disulfide-bonded Cys11 and Cys11′ side chains are shown in ball-and-stick representation. (B) SDS−PAGE of Arc variants. Lane 1, standards with molecular masses (kDa) indicated on the left. Lane 2, reduced Arc-NC11. Lane 3, oxidized Arc-NC11. Lane 4, mixture of wild-type Arc (lower band) and sc-Arc (Arc-L1-Arc; upper band). Lane 5, reduced sc-Arc-NC11. Lane 6, oxidized sc-Arc-NC11.

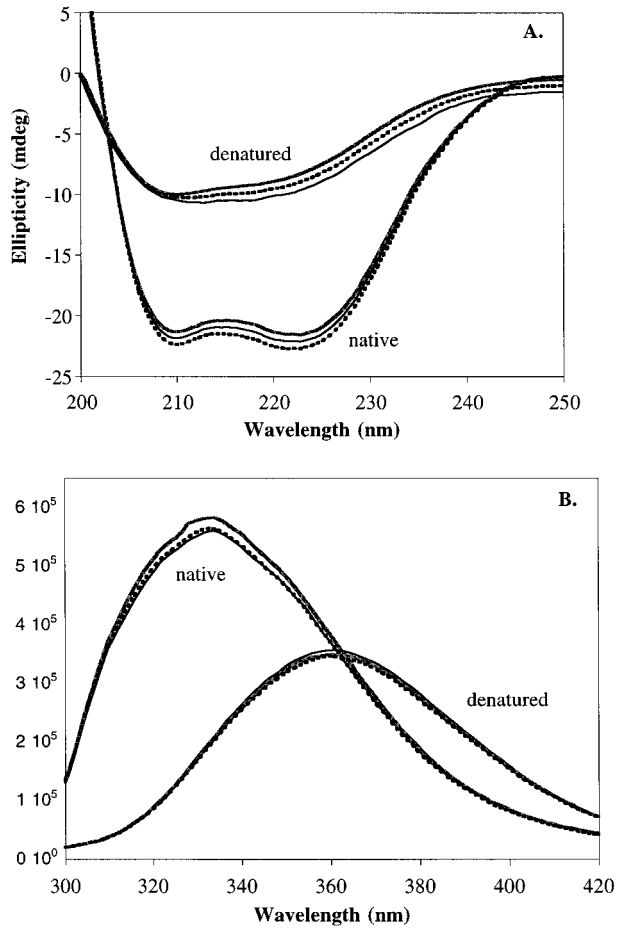

FIGURE 2: Spectroscopy of Arc variants (2.5 μM in subunit equivalents). Native spectra were taken in 50 mM Tris-HCl (pH 7.5), 250 mM KCl, and 0.1 mM EDTA. Denatured spectra were taken in the same buffer plus 6 M GuHCl. (A) Circular dichroism (CD) spectra: wild-type Arc, thin black line; sc-Arc-NC11 (oxidized), gray line; sc-Arc NC11 (reduced), dotted black line. (B) Fluorescence spectra: wild-type Arc, thin black line; sc-Arc-NC11 (oxidized), gray line; sc-Arc-NC11 (reduced), dotted black line.

RESULTS

Modeling and Disulfide Design. There are no cysteine residues in wild-type Arc. Computer searches using the program PROTEUS (*27*) and the crystal structure of an Arc dimer (*4*) identified three potential residue positions where a disulfide bond between the Arc subunits could be accommodated: (i) 11−11′ (see Figure 1A); (ii) 9−13′ and 9′−13; and (iii) 14−38′ and 14′−38. The first possibility offered the advantage of requiring only one cysteine per subunit, thereby minimizing the chances of competing intrasubunit disulfides, chaining of higher oligomeric forms, or other incorrect disulfide pairings. Moreover, the wild-type residues—Asn11 and Asn11′—are on the protein surface, and modeling suggested that a variety of Cys11 and Cys11′ side-chain conformations could form a disulfide cross-link without apparent strain or structural disruption.

Characterization of Native and Denatured States. Genes encoding the Asn11→Cys mutation were constructed in an otherwise wild-type background (Arc-NC11) and in the single-chain background (sc-Arc-NC11), and the corresponding proteins were expressed and purified. Following purification, both the reduced and disulfide-cross-linked species of each protein were detected by SDS−PAGE (Figure 1B). Dialysis in the absence of reducing agent converted each protein completely to the disulfide-cross-linked form. The disulfide-linked Arc-NC11 protein could be fully reduced by incubation with 100 mM DTT at 100 °C for 60 min at pH 2. Complete reduction of the oxidized sc-Arc-NC11 protein required 8 M urea in addition to 100 mM DTT at 100 °C for 60 min at pH 2.

Arc-NC11 and sc-Arc-NC11, in both their reduced and their oxidized forms, had circular dichroism (CD) and fluorescence spectra similar to the parent molecules. The denatured forms of the NC11 proteins also had spectral properties similar to their wild-type counterparts. For example, the center of fluorescence spectral mass decreased from ≈339 nm (≈29 500 cm^{-1}) for the native proteins to ≈357 nm (28 000 cm^{-1}) for the GuHCl denatured proteins. Similarly, thermal denaturation of each protein was accompanied by a loss of approximately 50% of the CD signal at 222 nm. Figure 2 shows spectra for wild-type Arc, and the reduced and oxidized forms of sc-Arc-NC11.

DNA Binding. The disulfide-cross-linked forms of Arc-NC11 and sc-Arc-NC11 bound to the *arc* operator in gel-mobility shift assays but with half-maximal concentrations roughly 100-fold higher than the wild-type controls (data not shown). Neither Arc-NC11 nor sc-Arc-NC11 passed a selection for Arc repressor activity in vivo. The reduced

Table 1: Equilibrium Stability [250 mM KCl, 0.2 mM EDTA, and 50 mM Tris-HCl (pH 7.5) or 50 mM Sodium Acetate (pH 2.0)][a]

		Arc (10 μM)	Arc-NC11 reduced (10 μM)	sc-Arc	sc-Arc-NC11 reduced	Arc-NC11 oxidized	sc-Arc-NC11 oxidized
ΔG_u (kcal/mol)[b]	at 25 °C	10.3 (±0.4)	12.3 (±0.9)	6.4 (±0.3)	8.7 (±0.8)	14.6 (±0.6)	17.2 (±0.5)
K_u (M or no units)[b]	at 25 °C	2.6 (±1.3) $\times 10^{-8}$ M	8.8 (±6.9) $\times 10^{-10}$ M	1.9 (±0.8) $\times 10^{-5}$	3.9 (±2.9) $\times 10^{-7}$	1.8 (±1.1) $\times 10^{-11}$	2.2 (±1.3) $\times 10^{-13}$
C_m[GuHCl] (M)	at 25 °C	1.1 (±0.1)	1.8 (±0.2)	2.1 (±0.1)	2.8 (±0.2)	4.7 (±0.1)	5.4 (±0.1)
m [kcal/(mol·M)]	at 25 °C	3.0 (±0.2)	3.0 (±0.2)	3.1 (±0.2)	3.1 (±0.1)	3.1 (±0.1)	3.2 (±0.3)
T_m (°C), pH 7.5		53.5 (±0.3)[c]	55.6 (±0.2)	69.8 (±0.2)[b]	70.7 (±0.1)	97.1 (±0.3)	>100
ΔH_u (kcal/mol), pH 7.5	at T_m	57 (±2)	59 (±3)	72 (±4)	77 (±5)	103 (±7)	>120
T_m (°C), pH 2		nd	nd	34 (±1)	nd	66.5 (±0.1)	99 (±1)
ΔH_u (kcal/mol), pH 2	at T_m	nd	nd	30 (±7)	nd	74 (±3)	111 (±9)

[a] Uncertainties represent 95% confidence levels based on nonlinear least-squares fitting of experimetal data. [b] Constants calculated from GuHCl denaturation. [c] Data from Robinson and Sauer (*18*). nd: not determined.

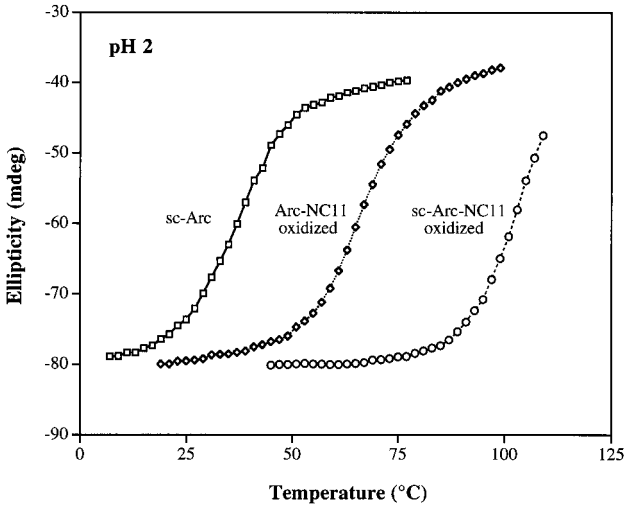

FIGURE 3: Thermal denaturation at pH 2 monitored by changes in CD ellipticity at 222 nm. Experiments were performed at protein concentrations of 10 μM (subunit equivalents) in 50 mM sodium acetate (pH 2.0), 250 mM KCl, 0.2 mM EDTA.

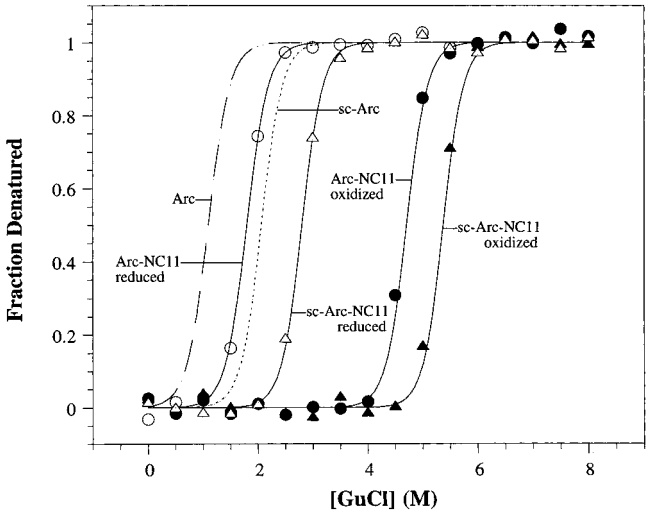

FIGURE 4: GuHCl denaturation monitored by changes in the intrinsic fluorescence (center of spectral mass) after excitation at 280 nm. Denaturation of 10 μM protein (subunit equivalents) was performed at 25 °C in buffer containing 50 mM Tris-HCl (pH 7.5), 250 mM KCl, 0.1 mM EDTA, and the indicated concentration of denaturant. The experimental data for Arc-NC11 (reduced), Arc-NC11 (oxidized), sc-Arc-NC11 (reduced), and sc-Arc-NC11 (oxidized) are shown as open or closed symbols, and the theoretical fits are shown as solid lines. For comparison, the dashed and dotted lines represent the denaturation profiles for 10 μM wild-type Arc and sc-Arc taken from Robinson and Sauer (*18*).

activity of these mutants was anticipated as the wild-type Asn11 side chain plays an important role in operator recognition (*4, 28*). The NA11 mutant of Arc also binds operator at approximately 100-fold higher concentrations than wild type and is inactive in vivo (*28*; B. M. Brown, unpublished), consistent with the idea that the decreased activity of the disulfide-bonded proteins arises from the loss of Asn11 and not from structural distortions introduced by the Cys11−Cys11′ disulfide bond.

Equilibrium Stability. The disulfide-bonded forms of Arc-NC11 and sc-Arc-NC11 were remarkably stable to thermal denaturation (Table 1; Figure 3). At neutral pH, where wild-type Arc (10 μM) and sc-Arc have T_m's of 53 and 69 °C, respectively, oxidized Arc-NC11 had an apparent T_m of 97 °C and disulfide-bonded sc-Arc-NC11 was still predominantly native at 99 °C. At pH 2, where wild-type Arc (10 μM) is unfolded and sc-Arc has a T_m of 34 °C, disulfide-bonded Arc-NC11 had a T_m of 66 °C, and disulfide-bonded sc-Arc-NC11 had an apparent T_m of 99 °C (Figure 3). As expected, the T_m's of disulfide-linked Arc-NC11, of reduced sc-Arc-NC11, and of oxidized sc-Arc-NC11 were independent of protein concentration (data not shown).

Denaturation by guanidine hydrochloride was also used to measure the stabilities of the Arc-NC11 and sc-Arc-NC11 mutants in both their reduced and their oxidized forms (Figure 4; Table 1). In the reduced state, Arc-NC11 and sc-Arc-NC11 were about 2 kcal/mol more stable than wild-type Arc and sc-Arc, respectively, indicating that the Asn11→Cys substitution is inherently stabilizing. In the disulfide-bonded state, Arc-NC11 and sc-Arc-NC11 were 7.8 and 10.8 kcal/mol more stable than sc-Arc, respectively, although these comparisons involve the effects of the NC11 mutations and/or the L1 peptide tether as well as the disulfide bond. The simplest comparison that involves just the effects of the disulfide is between the reduced and oxidized forms of sc-Arc-NC11, which differ in stability by 8.5 kcal/mol. The dependence of ΔG_u on guanidine concentration was similar for all proteins [m-values of 3.0−3.2 kcal/(mol·M); Table 1], indicating that similar changes in accessible surface area accompany all of the denaturation reactions (*29*−*31*).

Stability to Reduction. Equilibrium constants (K_{ex}) were determined for the disulfide−sulfhydryl exchange reactions between the reduced and oxidized forms of glutathione and the reduced and oxidized forms of denatured Arc-NC11 or

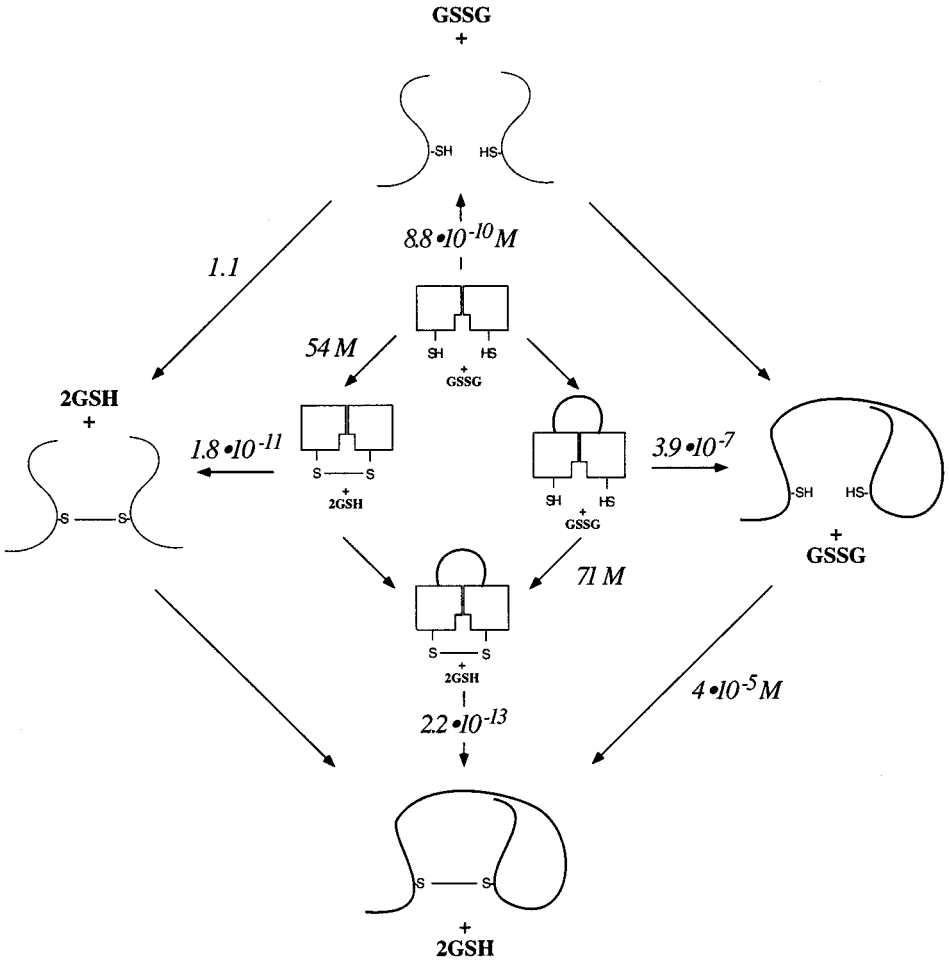

FIGURE 5: Thermodynamic cycles relating denaturation and oxidation/reduction of Arc-NC11 and sc-Arc-NC11. The inner cycle shows native proteins. The outer cycle shows denatured proteins (6 M GuHCl). The equilibrium constants for denaturation reactions (inner to outer species) are taken from Table 1. The equilibrium constants for the oxidation/reduction reactions of the denatured proteins are taken from the experiments described in the text; oxidation/reduction of the native proteins could not be measured directly, and the constants shown were calculated from the other equilibrium constants in each cycle. The reaction steps with no equilibrium constants represent covalent linkage of two Arc subunits with the 15-residue L1 linker to generate single-chain Arc (*24*). GSSG, oxidized glutathione. GSH, reduced glutathione.

sc-Arc-NC11. For denatured Arc-NC11, K_{ex} was 1.1, indicating that the Cys11−Cys11′ disulfide in this denatured protein has roughly the same stability as the disulfide in oxidized glutathione. For denatured sc-Arc-NC11, K_{ex} was 40 μM, a value significantly lower than the values of 0.5−100 mM found for disulfides in other denatured monomeric proteins (*26*, *32*, *33*). This indicates that the Cys11−Cys11′ disulfide in denatured sc-Arc-NC11 is more easily reduced than other disulfides that have been studied.

The K_{ex} values discussed above can be considered to be effective concentrations (C_{eff-D}) for the Cys11−Cys11′ disulfide bond in the denatured state (*32*). The Cys11−Cys11′ disulfide in native Arc-NC11 and in sc-Arc-NC11 was too stable to determine K_{ex} or C_{eff-N} values directly, but these values could be calculated from the thermodynamic cycle shown in Figure 5. This analysis assumes that the C_{eff-D} values are independent of denaturant concentration (see refs *26* and *33*) and gives C_{eff-N} values of 54 M for Arc-NC11 and 71 M for sc-Arc-NC11. Hence, the native disulfides have roughly comparable stabilities in the single-chain and dimeric backgrounds.

Unfolding and Refolding Rates. Unfolding rates were measured by denaturant−jump experiments for the disulfide-bonded forms of the Arc-NC11 and sc-Arc-NC11 proteins (Table 2; Figure 6A,B). Linear extrapolations of the log(k_u) versus denaturant plots predict a half-life in the absence of denaturant of approximately 100 days for disulfide-bonded Arc-NC11 and a half-life of approximately 13 days for disulfide-bonded sc-Arc-NC11. For comparison, the half-lives of unfolding for sc-Arc and wild-type Arc range from 1 to 10 s under the same conditions (*18*). Hence, the Cys11−Cys11′ disulfide bond seems to decrease the unfolding rate in the absence of denaturant by a factor of roughly 1.5×10^6 relative to the reduced proteins. One caveat, however, is that curvature in log(k_u) versus denaturant plots for Arc can lead to errors in the calculated unfolding rate in the absence of denaturant (*34*). To minimize potential errors of this type, the unfolding rate of the disulfide-bonded Arc-NC11 variant was also compared with that of wild-type Arc at a reference concentration of 5 M GuHCl using data for wild-type Arc unfolding from Schildbach et al. (*9*). Under these conditions, k_u was 2×10^{-3} s^{-1} for oxidized Arc-NC11 and 4×10^2 s^{-1} for wild-type Arc, indicating that the disulfide-bonded protein unfolds approximately (2×10^5)-fold more slowly than wild type.

Table 2: Kinetics of Unfolding and Refolding [25 °C, 50 mM Tris-HCl (pH 7.5), 250 mM KCl, 0.2 mM EDTA][a]

	Arc(10 μM)	sc-Arc	Arc-NC11 oxidized	sc-Arc-NC11 oxidized
k_{f-app} (s^{-1}), no GuHCl	1.0 ($\pm$0.15) $\times$ 10^2 [b]	10.4 ($\pm$1.4) $\times$ 10^3 [b]	3.1 ($\pm$0.2) $\times$ 10^3	1.7 ($\pm$0.6) $\times$ 10^6
k_u (s^{-1}), no GuHCl	0.11 ($\pm$0.03)[b]	1.1 ($\pm$0.1)[b]	8.1 ($\pm$0.5) $\times$ 10^{-8}	6.0 ($\pm$0.3) $\times$ 10^{-7}
k_u (s^{-1}), 5 M GuHCl	2.7 ($\pm$0.6) $\times$ 10^3 [c]	2.5 ($\pm$0.7) $\times$ 10^4	2.0 ($\pm$0.2) $\times$ 10^{-3}	1.6 ($\pm$0.4) $\times$ 10^{-2}
m_f	$-$1.77 ($\pm$0.04)	$-$1.64 ($\pm$0.06)	$-$1.94 ($\pm$0.03)	$-$1.85 ($\pm$0.07)
m_u	0.91 ($\pm$0.05)	0.82 ($\pm$0.09)	1.18 ($\pm$0.05)	1.19 ($\pm$0.07)
$m_f/(m_f - m_u)$	0.66 ($\pm$0.06)	0.66 ($\pm$0.09)	0.62 ($\pm$0.04)	0.61 ($\pm$0.07)

[a] Uncertainties represent 95% confidence levels based on nonlinear least-squares fitting of experimetal data. [b] Data from Robinson and Sauer (*18*). [c] Data from Schildbach et al. (*9*). For Arc, $k_f = k_{f-app}/(10^{-5}\ M) = 10^7\ M^{-1}\ s^{-1}$. For the single-chain and/or oxidized Arc variants, $k_{f-app} = k_f$.

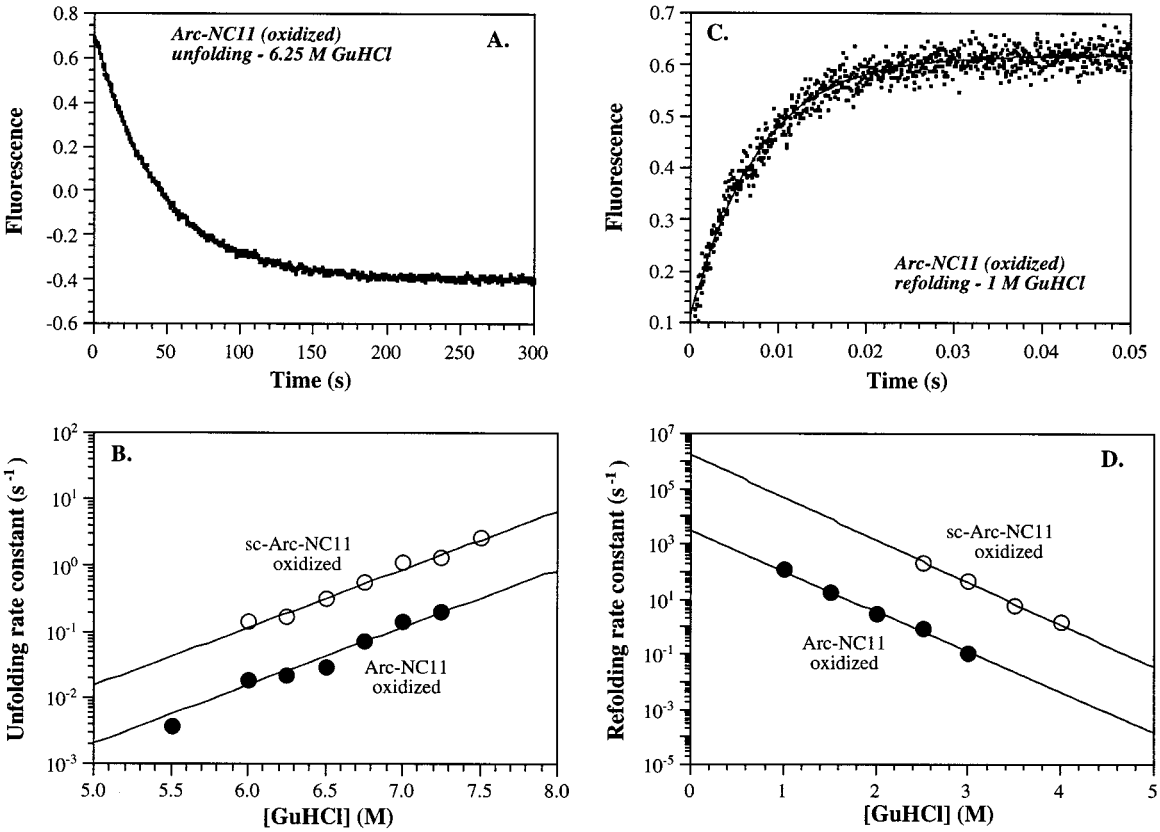

FIGURE 6: Unfolding and refolding kinetics performed at 25 °C in buffers containing 50 mM Tris-HCl (pH 7.5), 250 mM KCl, 0.1 mM EDTA, and different amounts of GuHCl. (A) Unfolding trajectory for 6.1 μM Arc-NC11 (oxidized) following a jump from 2.5 to 6.25 M GuHCl. The solid line is the fit to a single exponential with a rate constant of 0.023 s^{-1}. (B) Denaturant dependence of the unfolding rate constants for the disulfide-bonded forms of Arc-NC11 and sc-Arc-NC11. The solid lines are linear least-squares fits. (C) Refolding trajectory for 4.7 μM Arc-NC11 (oxidized) following a jump from 6 to 1 M GuHCl. The solid line is a single-exponential fit with a rate constant of 130 s^{-1}. (D) Denaturant dependence of the refolding rate constants for the disulfide-bonded forms of Arc-NC11 and sc-Arc-NC11. The solid lines are linear least-squares fits.

Refolding rates were also determined by denaturant−jump experiments for the disulfide-bonded Arc-NC11 and sc-Arc-NC11 proteins (Table 2; Figure 6C,D). Extrapolation of the log(k_f) versus GuHCl data gave a refolding rate constant of $3.1 \times 10^3\ s^{-1}$ for disulfide-bonded Arc-NC11 and $1.7 \times 10^6\ s^{-1}$ for the disulfide-bonded sc-Arc-NC11 molecule. The latter rate constant corresponds to a folding half-life of less than 1 μs. For comparison, the zero-denaturant refolding rate constant is $10^4\ s^{-1}$ for sc-Arc (*18*). Thus, in the context of the sc-Arc protein, the Cys11−Cys11′ disulfide accelerates refolding by approximately 170-fold.

The solvent accessibility of the transition state can be estimated from the denaturant dependence of the refolding and unfolding rates (*29*, *35*). The m_f and m_u values were slightly greater for the disulfide-bonded Arc-NC11 and sc-Arc-NC11 mutants than for wild-type Arc, but similar estimates of burial of hydrophobic surface (61−66%) were obtained for the transition states of all three proteins (Table 2).

DISCUSSION

A designed disulfide bond linking residues 11 and 11′ in the antiparallel β sheet of the Arc dimer was predicted to have good geometry using the PROTEUS algorithm of Pabo and Suchanek (*27*). We replaced the wild-type residue Asn11 with Cys and found that the Cys11−Cys11′ disulfide bond forms readily by air oxidation. Recent studies have shown that an Asn11→Leu substitution in Arc can lead to a structural change in which the β sheet is replaced by 3_{10} helices (*36*; M. Cordes and R. T. Sauer, unpublished), but two observations indicate that the Cys11−Cys11′ disulfide does not form in this alternative structure. First, the Arc structure with 3_{10} helices shows distinctive changes in both far-UV CD and fluorescence spectra, whereas the disulfide-

bonded Arc-NC11 and sc-Arc-NC11 proteins have spectra very similar to those of wild-type Arc. Second, the β carbons of residues 11 and 11′ are 12 Å apart in the 3_{10} helical conformation and could not form a disulfide without major structural rearrangements.

The NC11 substitution stabilizes Arc in both its reduced and its oxidized forms. In the reduced state, Arc-NC11 is approximately 2.0 kcal/mol more stable than wild-type Arc as measured by GuHCl denaturation at 25 °C. Apparently, the wild-type Asn11 side chains make unfavorable contacts or the mutant Cys11 side chains make favorable interactions in the context of the wild-type β sheet. Previous studies showed that the NA11 mutation is also stabilizing by 1.5 kcal/mol (*25*), providing some support for the former possibility. The NC11 substitution was found to be less stabilizing in thermal than GuHCl denaturation studies, suggesting that $\Delta\Delta G_u$ for this mutant changes with temperature.

Cross-linking of the strands of the antiparallel β sheet by the Cys11−Cys11′ disulfide bond increased the stability of Arc to thermal and chemical denaturation in a dramatic fashion. In the single-chain background, this disulfide stabilized the protein by 8.5 kcal/mol and raised the melting temperature by approximately 40 °C to greater than 100 °C at neutral pH and to nearly 100 °C at pH 2. Although stabilizing effects of disulfides have been reported in many systems, the effects of the Cys11−Cys11′ disulfide in Arc are particularly striking. For example, based on the stabilities of naturally occurring disulfide bonds in lysozyme, RNase A, RNase T1, and immunoglobulins, Pace et al. (*37*) concluded: "*Thus, only in exceptional cases will a disulfide contribute more than 5 kcal/mol to the conformational stability of a globular protein.*" Indeed, the most successful engineered disulfide bonds heretofore have been stabilizing by only 3−4 kcal/mol (*10*, *15*−*17*). Even among naturally occurring disulfides, the stability afforded to Arc by the Cys11−Cys11′ disulfide bond is remarkable. To our knowledge, only the 5−55 disulfide bond in BPTI has been reported to be more stabilizing; this disulfide, which is buried in the protein core, has a $\Delta\Delta G_u$ value of 10.2 kcal/mol [calculated as: $-RT \ln(C_{eff-N}/C_{eff-D})$; ref *32*].

The contribution of a cross-link to protein stability can be expressed as an "effective concentration" or C_{eff} value, which represents the ratio of the equilibrium constants for otherwise comparable bimolecular and unimolecular reactions. For example, dividing the bimolecular equilibrium constant for protein unfolding for wild-type Arc by the corresponding unimolecular constant for sc-Arc gives C_{eff} values of approximately 1−3 mM (*18*). The stabilizing effects of disulfide cross-links in monomeric proteins can also be expressed as an effective concentration by measuring the equilibrium constant for the exchange reaction in which the protein disulfide is reduced and a disulfide is formed between two molecules of a reagent like glutathione (*32*, *26*). Native protein disulfides have effective concentrations of 10 M to 5×10^5 M, and disulfides in denatured proteins typically have effective concentrations of roughly 0.5−100 mM depending on loop size (*26*, *32*, *33*, *38*).

Why is the Cys11−Cys11′ disulfide bond in Arc so stabilizing? The C_{eff-N} for this bond in sc-Arc-NC11 is only 71 M, approximately 6000-fold lower than C_{eff-N} for the 5−55 disulfide of BPTI (*32*). This is reasonable as Cys11 is

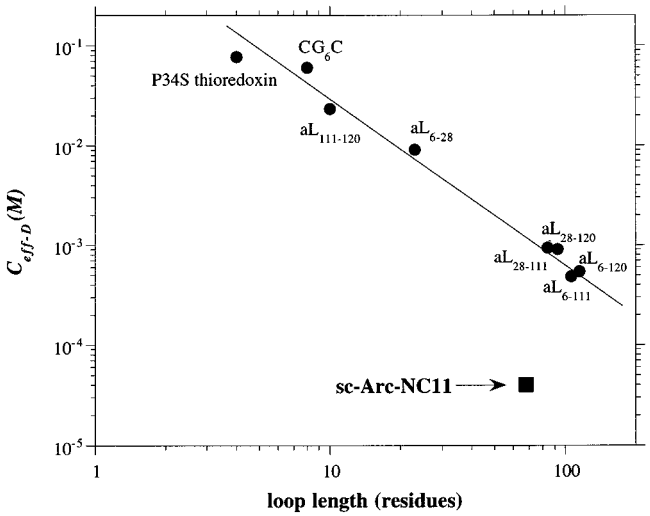

FIGURE 7: Disulfide bond in denatured Arc-sc-NC11 has an anomalously low effective concentration. C_{eff-D} values are plotted as a function of loop size for disulfide bonds in variants of α-lactalbumin (aL; ref *33*), the P34S mutant of thioredoxin (*38*), a CG_6C peptide (*26*), and the Cys11−Cys11′ disulfide of Arc-sc-NC11.

on the surface of Arc, whereas most disulfides with high C_{eff-N} values are highly constrained by burial in the protein core. Thus, the Cys11-Cys11′ disulfide must be hyper stabilizing because it has an abnormally low value of C_{eff-D}. Indeed, C_{eff-D} for the Cys11−Cys11′ disulfide in sc-Arc-NC11 is 40 μM, a value far lower than C_{eff-D} values measured for other proteins, even when the loop size between the Cys residues is taken into account (Figure 7). Apparently, one or more factors specific to single-chain Arc make it more difficult to form the disulfide in denatured sc-Arc-NC11 than in most denatured polypeptide chains. One possibility is that the non-native structure in the denatured state must be broken to bring Cys11 and Cys11′ together. By this model, formation of the Cys11−Cys11′ disulfide stabilizes single-chain Arc, in part, by reducing the stability of the denatured state. Such a model is consistent with our finding that residual structure in thermally denatured Arc subunits leads to a specific association of the denatured monomers (*6*). This situation provides an interesting contrast to cytochrome *c*, in which an engineered disulfide *destabilizes* the protein by increasing structure in the denatured state (*39*, *40*). Another possibility is that the low C_{eff-D} in sc-Arc-NC11 is caused by local charges around Cys11 that make forming a disulfide unfavorable. We view this theory as unlikely, however, as a charge effect would also be expected to reduce the stability of the disulfide in oxidized Arc-NC11 to reduction but this bond has a normal stability, comparable to that of the disulfide in oxidized glutathione.

It is formally possible that the presence of GuHCl perturbs the C_{eff-D} value measured for sc-Arc-NC11, but this is unlikely to account for the low C_{eff-D} value. First, C_{eff-D} values in other proteins have been shown to be independent of denaturant concentration (*26*). Second, GuHCl would be expected to disrupt structure in the denatured state, whereas the anomalously low C_{eff-D} value for sc-Arc-NC11 suggests residual non-native structure. Hence, if there were a denaturant effect on C_{eff-D} for sc-Arc-NC11, this would be expected to lower the physiological value even further.

The very slow rate of unfolding of disulfide-bonded sc-Arc relative to sc-Arc (10^5-10^6-fold) indicates that fastening the β strands with the Cys11−Cys11′ disulfide reinforces a relatively fragile region of structure. Indeed, the amide hydrogens in the wild-type β sheet exchange with solvent more rapidly than protons in the α helical portions of Arc, suggesting that structure in the β sheet may be transiently lost without global unfolding (*41*). Hydrogen bonding between the β strands is also known to be a late event in folding, and thus breaking these hydrogen bonds must be a prerequisite for unfolding (*9*). Finally, recent studies indicate that Arc bearing the NL11 mutation can switch between the β sheet and a helical form on the millisecond time scale (M. Cordes and R. T. Sauer, unpublished). All of these observations are consistent with the two-stranded β sheet in wild-type Arc being a metastable structure and help to explain why the Cys11−Cys11′ disulfide causes such a dramatic reduction in the rate of unfolding.

Stabilizing mutations that act before the transition state for refolding should accelerate refolding, whereas those that act after the transition state should slow unfolding. The Cys11−Cys11′ disulfide in sc-Arc-NC11 has both effects, but the latter is dominant. The refolding rate is enhanced by roughly 100-fold, whereas unfolding is slowed by roughly 5 orders of magnitude. One interpretation of these results is that some interactions involving proximity of the two β strands occur early while others occur late in refolding. This view is consistent with the effects of other mutations in Arc's β sheet. For example, the FA10 and LA12 mutations alter residues in the β sheet that contribute to Arc's hydrophobic core. These mutations slow refolding by 2−4-fold and accelerate unfolding by 16−22-fold (*42*). Again, the principal effects are on unfolding, but some early events in refolding also seem to be perturbed. For both of the core mutations in the β sheet and the disulfide, 20−35% of the net energetic effect of the mutations relative to wild type are evident before the transition state and 65−80% are manifest after the transition state. As mentioned earlier, however, the PL8 mutation which adds additional hydrogen bonds to Arc's β sheet appears to act only after the transition state. One possibility is that some hydrophobic packing between residues that will form the β sheet occurs early in the folding process, whereas more detailed packing interactions and formation of interstrand hydrogen bonds is a late event in folding.

The Cys11−Cys11′ disulfide and the 15-residue L1 peptide linker act together to stabilize the doubly cross-linked sc-Arc-NC11 variant. For example, inspection of the thermodynamic cycles shown in Figure 5 shows that the disulfide has almost the same $C_{\text{eff}-\text{N}}$ value in dimeric Arc and single-chain Arc, indicating that the stabilizing effects of the two cross-linkers are almost completely additive. We note, however, that there are few certainties when it comes to trying to stabilize proteins with engineered disulfides, anticipating the effects of natural disulfides on folding kinetics, or predicting whether disulfides and other types of cross-links will be mutually stabilizing. Thus, some engineered disulfides have been shown to be destabilizing (*39, 40*), formation of some natural disulfides slows refolding (*43*), and in BPTI formation of the wild-type disulfides and a chemical cross-link between the N- and C-termini are not mutually stabilizing (*44*). Nevertheless, the additive effects of the Cys11−Cys11′ disulfide and the L1 subunit linker in stabilizing Arc support the idea that extreme protein stability can be obtained by combining modestly stabilizing mutations (*11, 12*). How stable can Arc be made? It will be interesting to see whether addition of mutations such as PL8 and MYL, which are stabilizing by 2.5−4 kcal/mol in wild-type backgrounds (*9, 45*), will improve the stability of the disulfide-bonded sc-Arc-NC11 molecule. Moreover, the glycine-rich L1 linker could be replaced with longer, alanine-rich linkers that mediate effective concentrations that are almost 10 000-fold higher (*46*). While some improvements in Arc stability should be possible, we note that the disulfide-bonded sc-Arc-NC11 variant described here already folds at a rate that is predicted to be close to the diffusion-imposed limit (*47*). Thus, the effects of additional mutations that accelerate wild-type refolding, such as MYL or improved linkers, are far from obvious.

ACKNOWLEDGMENT

We thank Lena Nekludova for assistance implementing the PROTEUS algorithm, Dennis Rentzeperis and Anne Skaja Robinson for helpful advice, and Tania Baker and Jonathan King for the use of equipment.

REFERENCES

1. Sauer, R. T., Milla, M. E., Waldburger, C. D., Brown, B. M., and Schildbach, J. F. (1996) Sequence Determinants of Folding and Stability for the P22 Arc Repressor Dimer. *FASEB J. 10*, 42−48.
2. Breg, J. N., van Opheusden, J. H. J., Burgering, M. J. M., Boelens, R., and Kaptein, R. (1990) Structure of Arc Repressor in solution: evidence for a family of β-sheet DNA-binding proteins. *Nature 346*, 586−589.
3. Bonvin, A. M. J. J., Vis, H., Breg, J. N., Burgering, M. J. M., Boelens, R., and Kaptein, R. (1994) Nuclear Magnetic Resonance Solution Structure of the Arc Repressor Using Relaxation Matrix Calculations. *J. Mol. Biol. 236*, 328−341.
4. Raumann, B. E., Rould, M. A., Pabo, C. O., and Sauer, R. T. (1994) DNA Recognition by β-sheets in the Arc Repressor-Operator Crystal Structure. *Nature 367*, 754−757.
5. Bowie, J. U., and Sauer, R. T. (1989a) Equilibrium Dissociation and Unfolding of the Arc Repressor Dimer. *Biochemistry 28*, 7139−7143.
6. Robinson, C. R., Rentzeperis, D., Silva, J. R., and Sauer, R. T. (1997) Formation of a Denatured Dimer Limits the Thermal Stability of Arc Repressor. *J. Mol. Biol. 273*, 692−700.
7. Matthews, B. W., Nicholson, H., and Becktel, W. J. (1987) Enhanced protein thermostability from site-directed mutations that decrease the entropy of unfolding. *Proc. Natl. Acad. Sci. U.S.A. 84*, 6663−6667.
8. Vershon, A. K., Blackmer, K., and Sauer, R. T. (1986) Mutagenesis of the Arc Repressor Using Synthetic Primers with Random Nucleotide Substitutions. in *Protein Engineering* (Inouye, M., and Sarma, R., Eds.) pp 243−256, Academic Press, Orlando, FL.
9. Schildbach, J. F., Milla, M. E., Jeffrey, P. D., Raumann, B. E., and Sauer, R. T. (1995) Crystal Structure, Folding, and Operator Binding of the Hyperstable Arc Repressor Mutant PL8. *Biochemistry 34*, 1405−1412.
10. Matsumura, M., Becktel, W. J., Levitt, M., and Matthews, B. J. (1989a) Stabilization of phage T4 lysozyme by engineered disulphide bonds. *Proc. Natl. Acad. Sci. U.S.A. 86*, 6562−6566.
11. Matsumura, M., Signor, G., and Matthews, B. W. (1989b) Substantial increase of protein stability by multiple disulphide bonds. *Nature 342*, 291−293.

12. Mitchinson, C., and Wells, J. A. (1989) Protein engineering of disulfide bonds in subtilisin BPN′. *Biochemistry 28*, 4807−4815
13. Takagi, H., Takahashi, T., Momose, H., Inouye, M., Maeda, Y., Matsuzawa, H., and Ohta, T. (1990) Enhancement of the thermostability of subtilisin E by introduction of a disulfide bond engineered on the basis of structural comparison with a thermophilic serine protease. *J. Biol. Chem. 265*, 6874−6878.
14. Eder, J., and Wilmanns, M. (1992) Protein engineering of a disulfide bond in beta/alpha barrel protein. *Biochemistry 31*, 4437−4444.
15. Clarke, J., and Fersht, A. R. (1993) Engineered disulfide bonds as probes of the folding pathway of barnase: increasing the stability of proteins against the rate of denaturation. *Biochemistry 32*, 4322−4329.
16. Zhang, T., Bertelsen, E., and Alber, T. (1994) Entropic effects of disulfide bonds on protein stability. *Nat. Struct. Biol. 1*, 434−438.
17. Hinck, A. P., Truckses, D. M., and Markley, J. M. (1996) Engineered disulfide bonds in staphylococcal nuclease: effects on the stability and conformation of the folded protein. *Biochemistry 35*, 10328−10338.
18. Robinson, C. R., and Sauer, R. T. (1996a) Equilibrium Stability and Sub-Millisecond Refolding of a Designed Single-Chain Arc Repressor. *Biochemistry 35*, 13878−13884.
19. Sambrook, J., Fritsch, E. F., and Maniatis, T. (1989) *Molecular Cloning: A Laboratory Manual*, Cold Spring Harbor Press, Cold Spring Harbor, NY.
20. Milla, M. E., Brown, B. M, and Sauer, R. T. (1993) P22 Arc Repressor: Enhanced Expression of Unstable Mutants by Addition of Polar C-terminal Sequences. *Protein Sci. 2*, 2198−2205.
21. Sanger, F., Nicklen, S., and Coulson, A. R. (1977) DNA sequencing with chain-terminating inhibitors. *Proc. Natl. Acad. Sci. U.S.A. 74*, 5463−5469.
22. Bowie, J. U., and Sauer, R. T. (1989b) Identification of C-terminal Extensions That Protect Proteins from Intracellular Proteolysis. *J. Biol. Chem. 264*, 7596−7602.
23. Brown, B. M., and Sauer, R. T. (1993) Assembly of the Arc Repressor−Operator Complex: Cooperative Interactions between DNA-Bound Dimers. *Biochemistry 32*, 1354−1363.
24. Robinson, C. R., and Sauer, R. T. (1996b) Covalent Attachment of Arc Repressor Subunits by a Peptide Linker Enhances Affinity for Operator DNA. *Biochemistry 35*, 109−116.
25. Milla, M. E., Brown, B. M., and Sauer, R. T. (1994) Protein stability effects of a complete set of alanine substitutions in Arc repressor. *Nat. Struct. Biol. 1*, 518−523.
26. Lin, T.-Y., and Kim, P. S. (1989) Urea Dependence of Thio−Disulfide Equilibria in Thioredoxin: Confirmation of the Linkage Relationship and a Sensitive Assay for Structure. *Biochemistry 28*, 5282−5287.
27. Pabo, C. O., and Suchanek, E. G. (1986) Computer-Aided Model-Building Strategies for Protein Design. *Biochemistry 25*, 5987−5991.
28. Brown, B. M., Milla, M. E., Smith, T. L., and Sauer, R. T. (1994) Scanning Mutagenesis of Arc Repressor as a Functional Probe of Operator Recognition. *Nat. Struct. Biol. 1*, 164−168.
29. Tanford, C. (1970) Protein Denaturation Part C: Theoretical models for the mechanism of denaturation. *Adv. Protein Chem. 24*, 1−95.
30. Myers, J. K., Pace, C. N., and Scholtz, J. M. (1995) Denaturant *m* values and heat capacity changes: Relation to changes in accessible surface areas of protein unfolding. *Protein Sci. 4*, 2138−2148.
31. Wrabl, J., and Shortle, D. (1999) A model of the changes in denatured state structure underlying *m* value effects in staphylococcal nuclease. *Nat. Struct. Biol. 6*, 876−883.
32. Creighton, T. E., and Goldenberg, D. P. (1984) Kinetic role of a meta-stable nativelike two-disulphide species in the folding transition of bovine pancreatic trypsin inhibitor. *J. Mol. Biol. 179*, 497−526.
33. Peng, Z. Y., Wu, L., and Kim, P. S. (1995) Local structural preferences in the alpha-lactalbumin molten globule. *Biochemistry 34*, 3248−3252.
34. Jonsson, T., Waldburger, C. D., and Sauer, R. T. (1996) Nonlinear Free Energy Relationships in Arc Repressor Unfolding Imply Existence of Unstable, Nativelike Folding Intermediates. *Biochemistry 35*, 4795−4802.
35. Matouschek, A., and Fersht, A. R. (1993) Application of physical organic chemistry to engineered mutants of proteins: Hammond postulate behavior in the transition state of protein folding. *Proc. Natl. Acad. Sci. U.S.A. 90*, 7814−7818.
36. Cordes, M. J., Walsh, N., McKnight, J., and Sauer, R. T. (1999) Evolution of a Protein Fold In Vitro. *Science 284*, 325−327.
37. Pace, C. N., Grimsley, G. R., Thomson, J. A., and Barnett, B. J. (1988) Conformational stability and activity of ribonuclease T1 with zero, one, and two intact disulfide bonds. *J. Biol. Chem. 263*, 11820−11825.
38. Lin, T.-Y., and Kim, P. S. (1991) Evaluating the effects of a single amino acid substitution on both the native and denatured states of a protein. *Proc. Natl. Acad. Sci. U.S.A. 88*, 10573−10577.
39. Betz, S. F., and Pielak, G. J. (1992) Introduction of a disulfide bond into cytochrome *c* stabilizes a compact denatured state. *Biochemistry 31*, 12337−12344.
40. Betz, S. F., Marmorino, J. L., Saunders, A. J., Doyle, D. F., Young, G. B., and Pielak, G. J. (1996) Unusual effects of an engineered disulfide on global and local protein stability. *Biochemistry 35*, 7422−7428.
41. Burgering, M. J., Hald, M., Boelens, R., Breg, J. N., and Kaptein, R. (1995) Hydrogen exchange studies of the Arc repressor: evidence for a monomeric folding intermediate. *Biopolymers 35*, 217−226.
42. Milla, M. E., Brown, B. M., Waldburger, C. D., and Sauer, R. T. (1995) P22 Arc Repressor: Transition State Properties Inferred from Mutational Effects on the Rates of Protein Unfolding and Refolding. *Biochemistry 34*, 13914−13919.
43. Mücke, M., and Schmid, F. X. (1994) Intact disulfide bonds decelerate the folding of ribonuclease T1. *J. Mol. Biol. 239*, 713−725.
44. Goldenberg, D. P., and Creighton, T. E. (1984) Folding pathway of a circular form of bovine pancreatic trypsin inhibitor. *J. Mol. Biol. 179*, 527−545.
45. Waldburger, C. D., Schildbach, J. F., and Sauer, R. T. (1995) Are Buried Salt Bridges Important for Protein Stability and Conformational Specificity. *Nat. Struct. Biol. 2*, 122−128.
46. Robinson, C. R., and Sauer, R. T. (1998) Optimizing the Stability of Single-Chain Proteins by Linker Length and Composition Mutagenesis. *Proc. Natl. Acad. Sci. U.S.A. 95*, 5929−5934.
47. Hagen, S. J., Hofrichter, J., Szabo, A., and Eaton, W. A. (1996) Diffusion-limited contact formation in unfolded cytochrome *c*: estimating the maximum rate of protein folding. *Proc. Natl. Acad. Sci. U.S.A. 93*, 11615−11617.

BI001484E